



**AFRL-RX-WP-TP-2010-4066**

**TEMPLATED GROWTH OF HEXAGONAL NICKEL  
CARBIDE NANOCRYSTALS ON VERTICALLY ALIGNED  
CARBON NANOTUBES (PREPRINT)**

**J.Y. Hwang, A.R.P. Singh, M. Chaudhari, J. Du, and R. Banerjee**

**University of North Texas**

**J.S. Tiley**

**Metals Branch**

**Metals, Ceramics & NDE Division**

**Y. Zhu**

**North Carolina State University**

**JANUARY 2010**

**Approved for public release; distribution unlimited.**

*See additional restrictions described on inside pages*

**STINFO COPY**

**AIR FORCE RESEARCH LABORATORY  
MATERIALS AND MANUFACTURING DIRECTORATE  
WRIGHT-PATTERSON AIR FORCE BASE, OH 45433-7750  
AIR FORCE MATERIEL COMMAND  
UNITED STATES AIR FORCE**

REPORT DOCUMENTATION PAGE				Form Approved OMB No. 0704-0188	
The public reporting burden for this collection of information is estimated to average 1 hour per response, including the time for reviewing instructions, searching existing data sources, gathering and maintaining the data needed, and completing and reviewing the collection of information. Send comments regarding this burden estimate or any other aspect of this collection of information, including suggestions for reducing this burden, to Department of Defense, Washington Headquarters Services, Directorate for Information Operations and Reports (0704-0188), 1215 Jefferson Davis Highway, Suite 1204, Arlington, VA 22202-4302. Respondents should be aware that notwithstanding any other provision of law, no person shall be subject to any penalty for failing to comply with a collection of information if it does not display a currently valid OMB control number. PLEASE DO NOT RETURN YOUR FORM TO THE ABOVE ADDRESS.					
1. REPORT DATE (DD-MM-YY) January 2010		2. REPORT TYPE Journal Article Preprint		3. DATES COVERED (From - To) 01 January 2010 – 01 January 2010	
4. TITLE AND SUBTITLE TEMPLATED GROWTH OF HEXAGONAL NICKEL CARBIDE NANOCRYSTALS ON VERTICALLY ALIGNED CARBON NANOTUBES (PREPRINT)				5a. CONTRACT NUMBER In-house	
				5b. GRANT NUMBER	
				5c. PROGRAM ELEMENT NUMBER 62102F	
6. AUTHOR(S) J.Y. Hwang, A.R.P. Singh, M. Chaudhari, J. Du, and R. Banerjee (University of North Texas) J.S. Tiley (AFRL/RXLM) Y. Zhu (North Carolina State University)				5d. PROJECT NUMBER 4347	
				5e. TASK NUMBER RG	
				5f. WORK UNIT NUMBER M02R1000	
7. PERFORMING ORGANIZATION NAME(S) AND ADDRESS(ES) University of North Texas Center for Advanced Research and Technology and Department of Materials Science and Engineering, Denton, TX 76203			8. PERFORMING ORGANIZATION REPORT NUMBER AFRL-RX-WP-TP-2010-4066		
9. SPONSORING/MONITORING AGENCY NAME(S) AND ADDRESS(ES) Air Force Research Laboratory Materials and Manufacturing Directorate Wright-Patterson Air Force Base, OH 45433-7750 Air Force Materiel Command United States Air Force			Metals Branch (AFRL/RXLM) Metals, Ceramics & NDE Division Materials and Manufacturing Directorate WPAFB, OH 45433-7750 Air Force Materiel Command, United States Air Force ----- North Carolina State University Department of Materials Science and Engineering Raleigh, NC 27695		
			10. SPONSORING/MONITORING AGENCY ACRONYM(S) AFRL/RXLMD		
11. SPONSORING/MONITORING AGENCY REPORT NUMBER(S) AFRL-RX-WP-TP-2010-4066					
12. DISTRIBUTION/AVAILABILITY STATEMENT Approved for public release; distribution unlimited.					
13. SUPPLEMENTARY NOTES Journal article submitted to <i>Advanced Materials</i> . PAO Case Number: 88ABW-2009-5146; Clearance Date: 11 Dec 2009. Paper contains color.					
14. ABSTRACT Nanocrystals of hexagonal nickel carbide have been synthesized via physical vapor deposition of elemental nickel onto the surface of vertically aligned carbon nanotubes. Combining high resolution transmission electron microscopy (HRTEM) with three-dimensional atom probe tomography (3DAP) confirmed that these nanocrystals have a hexagonal structure, are enriched in carbon, and have a composition of ~Ni-25at%C (Ni <sub>3</sub> C). This metastable hexagonal nickel carbide phase appears to be stabilized due to the growth of the nanocrystals on the surface of the nanotubes that act as a template and also as a source of carbon. The stability of this nickel carbide phase has also been investigated by Density Functional Theory (DFT) calculations and compared to the experimental results.					
15. SUBJECT TERMS hybrid nanostructure, carbon nanotube, metal nanocrystal, hexagonal nickel atom probe tomography					
16. SECURITY CLASSIFICATION OF:			17. LIMITATION OF ABSTRACT: SAR	18. NUMBER OF PAGES 18	19a. NAME OF RESPONSIBLE PERSON (Monitor) Christopher F. Woodward 19b. TELEPHONE NUMBER (Include Area Code) N/A
a. REPORT Unclassified	b. ABSTRACT Unclassified	c. THIS PAGE Unclassified			

# Templated Growth of Hexagonal Nickel Carbide Nanocrystals on Vertically Aligned Carbon Nanotubes

J.Y. Hwang, A.R.P. Singh, M. Chaudhari, J. Tiley\*, Y. Zhu<sup>#</sup>, J. Du, and R. Banerjee

Center for Advanced Research and Technology and Department of Materials Science and Engineering, University of North Texas, Denton, TX 76203

\* Materials and Manufacturing Directorate, Air Force Research Laboratory, Dayton, OH, 45433

<sup>#</sup> Department of Materials Science and Engineering, North Carolina State University, Raleigh, NC 27695

## *Abstract*

Nanocrystals of hexagonal nickel carbide have been synthesized via physical vapor deposition of elemental nickel onto the surface of vertically aligned carbon nanotubes. Combining high-resolution transmission electron microscopy (HRTEM) with three-dimensional atom probe tomography (3DAP) confirmed that these nanocrystals have a hexagonal structure, are enriched in carbon, and have a composition of ~Ni-25at%C ( $\text{Ni}_3\text{C}$ ). This metastable hexagonal nickel carbide phase appears to be stabilized due to the growth of the nanocrystals on the surface of the nanotubes that act as a template and also as a source of carbon. The stability of this nickel carbide phase has also been investigated by Density Functional Theory (DFT) calculations and compared to the experimental results.

Keywords: Hybrid Nanostructure; Carbon Nanotube; Metal Nanocrystal; Hexagonal Nickel; Atom probe tomography.

Synthesis of nanocrystalline hybrid materials based on carbon nanotubes with metals or oxides has been of substantial interest in recent years due to their potential applications in bio sensing, energy storage, catalysis, electronic devices as well as structural applications [1-5]. For example, tin oxide ( $\text{SnO}_2$ ) nanocrystals deposited by an aero-gel process onto multi-walled carbon nanotubes have been found to be promising for gas-sensing applications at room temperatures [1] indicating that carbon nanotubes can be used as templates for deposition or growth of nanocrystals for various applications. Despite the various reports on synthesis of carbon nanotubes coated with nanocrystals, there have been rather limited high-resolution investigations of the structural and compositional details associated with these nanocrystals. Similarly there has

been a lot of interest in the synthesis of nanocrystalline metallic materials such as nickel, due to their application in a wide range of engineering fields, specifically catalysis, energy absorption, and magnetic recording media [6-8]. Elemental nickel, in its equilibrium form at room temperature exhibits a face centered cubic (FCC) structure. Interestingly, there have been reports in the literature related to the stabilization of a non-equilibrium hexagonal structure (hexagonal close-packed or HCP) in nanostructured forms of nickel, including HCP metastable nickel carbide nanocrystals [9-12]. The HCP phase is typically observed in case of far-from equilibrium synthesis routes such as wet chemical synthesis at very low temperatures when the nanocrystals grow from an amorphous phase [9], decomposition of neutral metal complex [10], thin film processing via hetero epitaxial growth [11], and mechanical alloying via high energy ball milling [12]. These synthesis methods indicate that HCP nickel is only observed below a certain critical crystallite size ( $\sim 4$  nm) and changes to the equilibrium FCC structure for larger crystallite sizes [9-10]. Nickel does not form a carbide under equilibrium conditions, however, there have been reports of metastable HCP nickel carbides ( $\text{Ni}_3\text{C}$ ) forming as a result of mechanical alloying in high energy ball-milled mixtures [12]. These HCP nickel carbide ( $\text{Ni}_3\text{C}$ ) nanocrystals also exhibited a highly disordered and defective internal structure due to extreme local pressures and temperatures involved in far-from equilibrium processing, such as high energy ball milling [12]. Furthermore, nanocrystals synthesized from a carbon-containing neutral metal complex of nickel, indicate that the HCP phase can be stabilized in much larger nanocrystals ( $\sim 20$  nm), possibly due to the presence of carbon [10]. However, a detailed investigation and clear understanding of the role of carbon on the stabilization of the HCP phase in nickel nanocrystals is presently lacking.

This paper reports the templated synthesis of hexagonal nickel carbide nanocrystals via physical vapor deposition (PVD) of elemental nickel onto the surface of double-walled carbon nanotubes. PVD processes such as sputter deposition offer a relatively simple and clean route for synthesizing nanocrystals on nanotube surfaces. Electron diffraction and high resolution transmission electron microscopy (HRTEM) was used to identify the crystal structure and morphologies, while three-dimensional atom probe tomography was used to determine the composition of the nickel carbide nanocrystals. The coupling of these two advanced characterization techniques permitted the determination of both the atomic scale structure and

composition of these nanocrystals for the first time. Furthermore, synergistic coupling of these experimental results with first-principles electronic structure based calculations of the relative energies of different metastable nickel and nickel carbide phases has led to a better insight into the role of carbon and the template offered by the nanotube surface on the formation of metastable nickel carbide nanocrystals.

## 2. Experiment

Using sputtering, elemental nickel was deposited onto vertically aligned CNT in a PVD system. Pure elemental Ni (99.99%) targets from Kurt Lesker Co., were used for the deposition. Si wafers with a high density of vertically grown CNTs on the surface were used as the substrate for the Ni deposition. A 10 mm x 10 mm piece of Si wafer, coated with the CNTs, was loaded into the PVD chamber and pumped down to a base pressure  $\sim 10^{-8}$  torr. Pure Argon sputtering gas was introduced into the chamber to achieve a working pressure  $\sim 5$  mTorr. Ni was deposited using the DC magnetron sputtering power at 200W at room temperature for 60 minutes. In order to characterize the nanostructured Ni deposited on the CNT surface, site-specific samples were prepared for both transmission electron microscopy (TEM) and 3D atom probe (3DAP) studies, using the FEI Nova 200 NanoLab – dual beam FIB instrument. In order to minimize the Gallium ion damage during the sample preparation, the area of interest was protected by depositing a Pt overlayer on the region of interest and subsequently lifting out samples. Lifted-out samples were attached to a copper grid for TEM studies. Additional thinning and cleaning to obtain less than 50 nm thickness using the FIB was done at 30 KeV and 5 KeV consequently to remove the redeposition and ion beam damage. The site specific samples have been characterized using the FEI Tecnai F20 field emission gun TEM operating at 200 kV. The sample for atom probe analysis was also prepared using the dual-beam FIB. 3DAP experiments were conducted on a LEAP 3000 Local Electrode Atom Probe (LEAP<sup>TM</sup>) microscope system manufactured by Imago Scientific Instruments, Inc. The laser-pulse evaporation method was used for analyzing these samples at a temperature of 60K with 0.5% average evaporation rate and a laser pulse energy of 0.5 nJ.

### 3. Results and Discussion

Fig. 1(a) shows a scanning electron microscopy (SEM) image on the as-received vertically aligned carbon nanotubes grown by chemical vapor deposition method on a Si wafer. The high density of aligned CNTs have a double-walled structure with a diameter  $\sim 4$  nm and length  $\sim 650$   $\mu\text{m}$  length. The detailed properties of these nanotubes are reported elsewhere [13]. Fig. 1(b) shows a SEM image from the nickel-coated carbon nanotubes, clearly exhibiting the granular morphology of nanocrystals uniformly coating the surface of the nanotubes (higher magnification shown as an inset). From bright-field TEM images, such as the representative one shown in Fig. 1(c), the average crystalline size was determined to be  $\sim 5$  nm. The electron diffraction, comprising multiple rings, shown as an inset in Fig. 1(c), confirmed the polycrystalline nature of the vapor deposited nanocrystals on the surface of the nanotubes.

For a detail analysis of morphology and crystal structure of these nanocrystals, an HRTEM image as well as an enlarged selected area diffraction (SAD) pattern are shown in Figs. 2(a) and (b) respectively. Fig. 2(a) clearly shows the formation of nanocrystals of relatively uniform size on the surface of the nanotubes, with the underlying graphene layers visible in some cases. The nanocrystals were typically less than  $\sim 3$  nm in size. Most of the primary rings observed in the SAD pattern shown in Fig. 2(b) can be consistently indexed based on a hexagonal (HCP) structure with a single weak ring corresponding to the face-centered cubic (FCC) structure of Ni. The lattice parameter of the HCP phase was determined to be  $a = 2.6$  ,  $c = 4.3 \text{ \AA}$  and found to be in close agreement with those reported previously by Tian et. al for hexagonal nickel nanocrystals [11] as well as by Yue et. al. for metastable  $\text{Ni}_3\text{C}$  nanocrystals [12]. The equilibrium phase diagram does not exhibit either any hexagonal Ni or nickel carbide phase. It appears that the carbon nanotubes can affect the formation of this hexagonal nickel phase by providing a template for heterogeneous nucleation during the physical vapor deposition process. Fig. 2(c) shows a relatively large Ni nanocrystal ( $\sim 20$  nm) on the CNT surface exhibiting a hexagonal structure as revealed by the corresponding  $[\bar{1}2\bar{1}3]$  zone axis SAD pattern (inset in Fig. 2(c)). The evidence of a hexagonal structure in this relatively large nanocrystal contradicts the critical size ( $\sim 4$  nm) of FCC-HCP transition reported previously for Ni nanocrystals by Illy et al. [9].

Figs. 3(a) and 3(b) are SEM images, respectively showing the lift-out procedure and the sample prepared for 3DAP studies of the Ni nanocrystals deposited on the carbon nanotubes. The lifted-out sample was attached on a Si micropillar, and then subsequently milled using the Ga ion beam with a final tip radius less than 30nm as shown in Fig. 3(b). The 3DAP sample preparation using FIB was well described elsewhere [14]. Fig. 3(c) shows a 3D atom probe reconstruction of the sample shown in Fig. 3(b). The C atoms have been plotted as red (color online) dots along with a solid isoconcentration surface (isosurface in short) in blue (color online) for Ni=50at%. Even though the Ni isosurface shows a clear interface between the Ni nanocrystal and CNT sides, the composition profiles across the nickel and CNT interface, plotted in Fig. 3(d), exhibit substantial intermixing between the two regions. The average composition of carbon in the Ni coated area (nickel nanocrystals) is ~25 at.%, which corresponds to ~Ni<sub>3</sub>C stoichiometry (refer Fig. 3(d)). Interestingly, while the metastable Ni<sub>3</sub>C phase has been proposed to form in high-energy ball-milled nanocrystalline nickel samples, there was no compositional evidence presented in support of this argument [12]. However, the reported HCP crystal structure and lattice parameters for this metastable carbide are in good agreement with the results of the present study. Yue et. al suggested carbon seems to be a significant role on the stabilization of HCP Ni phase, especially at lower growth temperatures. The present study suggest that hexagonal Ni<sub>3</sub>C nanocrystals can be stabilized up to sizes as large as ~20nm when grown on the surface of carbon nanotubes. Therefore, it appears that the nanotubes not only provide a template for the growth of the hexagonal nickel phase but also increase the stability of this phase due to the diffusion of carbon from the nanotubes into the nanocrystals. Under these circumstances it becomes imperative to investigate the relative stabilities of HCP Ni and HCP Ni<sub>3</sub>C phases with respect to the equilibrium FCC Ni phase. Such an analysis has been carried out using density functional theory (DFT) as described below.

We have performed plane wave Density Functional Theory (DFT) total energy calculations of HCP and FCC Ni, as well as orthorombic (cementite) and HCP Ni<sub>3</sub>C [16]. Equation of states of these structures were obtained by calculating the total energy versus volume curves with unit cell volumes spanning 10% up and below those of the experimental structures. The cell shape and atom positions were fully relaxed within the theory of DFT at each of the volumes. The final equation of states curves are shown in Fig. 4. Generalized gradient exchange correlation

functionals with the PBE form [17] and Projected Augmented Wave (PAW) [18] pseudopotentials to describe the electron - ion core interactions were used in the DFT calculations as implemented in the Vienna *ab initio* Simulation Package (VASP) [19-20]. Ni 3s and 3p electrons were treated as valence electrons ( $3s^2p^6d^84s^2$ ). Plane wave kinetic energy cutoff of 400 eV and 9x9x9 for Ni<sub>3</sub>C and 21x21x21 for Ni K-point sampling of Brillouin zone were used in the calculations. Geometry optimizations were performed using the conjugate gradient method until forces acting on each atom being smaller than 0.01 eV/Å. Spin polarized calculations were employed in all geometry optimization and energy calculations due to the magnetic nature of Ni. HCP Ni<sub>3</sub>C was found to have zero magnetization but both HCP and FCC Ni exhibited ferromagnetic behavior with residual magnetic moments of 0.63  $\mu_B$ .

DFT calculations show that the FCC Ni is more stable than HCP Ni by 0.024 eV/atom at equilibrium geometry, consistent with experiments and previous DFT calculations and verifies that spin polarized calculations are important in nickel and related systems [22]. In Fig. 4, in order to be comparable to the Ni<sub>3</sub>C equation of state, the energies and volumes of HCP and FCC Ni are plotted for three Ni atoms and the energy was shifted by adding the energy per atom of carbon (in the diamond structure) from calculations of the same conditions (-9.110 eV/atom). The orthorhombic cementite structured Ni<sub>3</sub>C equation of state was also calculated (not shown) and it is found that it has a higher energy than the HCP structure by 0.157 eV per Ni<sub>3</sub>C unit which is in good agreement with experimental observations of the existence of only hexagonal Ni<sub>3</sub>C. The energy versus volume curves were fitted to Birch–Murnaghan equation of state and equilibrium volume, cell parameter and bulk modulus were obtained. For hexagonal Ni<sub>3</sub>C, the equilibrium volume obtained from equation of state is about 2.82% larger than the experimental volume determined using electron diffraction and the corresponding unit cell sizes are 0.93% larger. The bulk modulus from equation of state is 188.2 GPa for Ni<sub>3</sub>C. The equilibrium Ni<sub>3</sub>C structure was used to calculate the electron diffraction patterns. The calculated TEM pattern agrees well with experimental data both in terms of the general hexagonal symmetry and the interatomic spacing of the planes in the diffraction pattern as shown in Table 1.

The formation of hexagonal Ni<sub>3</sub>C can become favorable in the consideration of total energy of the Ni/CNT systems based on our DFT calculations. The energy difference between the HCP Ni

+ carbon and the hexagonal  $\text{Ni}_3\text{C}$  is 0.063 eV/ $\text{Ni}_3\text{C}$  unit. Here the energy of carbon used for adding to the HCP Ni value is for the diamond structure, which compared to graphite is lower by 0.0197 eV/atom. However, due to the fact that in this case the carbon atoms are in the form of a nanotube, the total energy of carbon can be considerably higher than that of diamond or graphite. It was found from DFT calculations that the energy of formation of carbon nanotubes increases with decreasing tube diameters [23]. This will shift the equation of state for FCC and HCP Ni + C to a higher energy level, which will eventually favor the formation of HCP  $\text{Ni}_3\text{C}$  nanocrystals rather than HCP Ni nanocrystals on the surface of the CNTs. Furthermore, interfacial energy considerations are also likely to aid in the stabilization of the HCP  $\text{Ni}_3\text{C}$  nanocrystals.

Sputter deposition of elemental Ni onto vertically-aligned carbon nanotubes results in the templated nucleation and growth of  $\text{Ni}_3\text{C}$  nanocrystals exhibiting a hexagonal crystal structure. The nanotubes not only act as a template for the synthesis of these nanocrystals but also act as a source of carbon. The hexagonal phase can be stabilized in these nanocrystals to relatively large sizes ( $\sim 20$  nm). Density functional theory calculations indicate that the HCP  $\text{Ni}_3\text{C}$  phase is metastable with respect to FCC Ni + C (in diamond). However, the total energy difference between HCP  $\text{Ni}_3\text{C}$  and HCP Ni + C (in diamond) is relatively small and it is quite likely that the HCP  $\text{Ni}_3\text{C}$  phase might have a lower energy than HCP Ni + C (in nanotubes), resulting in their stabilization on the nanotube surface.

#### *Acknowledgements*

This work was financially supported by U. S. Air Force Research Laboratory (AFRL ISES contract) and the U. S. Air Force Office of Scientific Research (AFOSR Grant # FA9550-06-1-0193). The authors also gratefully acknowledge the Center for Advanced Research and Technology (CART) at the University of North Texas.

- [1] G. Lu, L.E. Ocola, and J. Chen, *Adv. Mater.* 21, 1 (2009).
- [2] D.S. Kim, S.M. Lee, R. Scholz, M. Knez, U. Gösele, J. Fallert, H. Kalt, and M. Zacharias, *Appl. Phys. Lett.* 93, 103108 (2008).
- [3] L. Zhu, G. Lu, and, J. Chen, *J. Heat Transfer*, **130**, 044502-1 (2008).
- [4] E.J. Garcia, A.J. Hart, B.L. Wardle, and A.H. Slocum, *Adv. Mater.* 19, 2151 (2007).
- [5] K. Ota, A. Kawabata, H. Murakami, E. Kita, *Mater. Trans*, 42, 1684 (2001).
- [6] N. Cordente, M. Respaud, F. Senocq, M.J. Casanove, C. Amiens, and B. Chaudret, *Nano Lett.* 1, 565 (2001).
- [7] J.C. Bao, C.Y. Tie, Z. Xu, Q.F. Zhou, D. Shen, Q. Ma, *Adv. Mater.* 13, 1631 (2001).
- [8] Z.P. Liu, S. Li, Y. Yang, S. Peng, Z.K. Hu, Y.T. Qian, *Adv. Mater.* 15, 1946 (2003).
- [9] S. Illy, O. Tillement, F. Machizud, J.M. Dubois, F. Massicot, Y. Fort, and J. Ghanbaja, *Phil. Mag. A*, 79, 1021 (1999).
- [10] V. Rodriguez-Gonzalez, E. Marceau, P. Beaunier, M. Che, C. Train, *J. Solid State Chem.* 180, 22 (2007).
- [11] W. Tian, H.P. Sun, X.Q. Pan, J.H. Yu, M. Yeadon, C.B. Boothroyd, Y.P. Feng, R.A. Lukaszew, and R. Clarke. *Appl. Phys. Lett.* 86, 131915 (2005).
- [12] L. Yue, R. Sabiryanov, E.M. Kirkpatrick, D.L. Leslie-Pelecky, *Phys. Rev. B.* 62, 8969 (2000).
- [13] X. Zhang, Q. Li, Y. Tu, Y. Li, J. Y. Coulter, L. Zheng, Y. Zhao, Q. Jia, D.E. Peterson, Y. Zhu, *Small*, 3, 244 (2007).
- [14] K. Thompson, D. Lawrence, D.J. Larson, J.D. Olson, T.F. Kelly, and B. Gorman, *Ultramicroscopy*, 107, 131 (2007).
- [15] M.K. Miller, K. R. Russell, K. Thompson, R. Alvis, and D.J. Larson, *Microsc. Microanal.* 13, 428 (2007).
- [16] S. Nagakura, *J. Phys. Soc. Jpn.* 13, 1005 (1958).
- [17] G. Kresse and J. Hafner, *Phys. Rev. B*, 49, 14251 (1994).
- [18] G. Kresse and J. Furthmüller, *Phys. Rev. B*, 54, 11169 (1996).
- [19] J. P. Perdew, K. Burke, and M. Ernzerhof, *Phys. Rev. Lett.*, 77, 3865 (1996).
- [20] P. E. Blochl, *Phys. Rev. B*, 50, 17953 (1994).
- [21] G. Kresse and D. Joubert, *Phys. Rev. B*, 59, 1758 (1999).
- [22] G. Y. Guo and H. H. Wang, *Chin. J. Physics*, 38, 949 (2000).
- [23] M.F. Budyka, T.S. Zyubina, A.G. Ryabenko, S.H. Lin, A.M. Mebel, *Chem. Phys. Lett.* 407, 266, (2005).

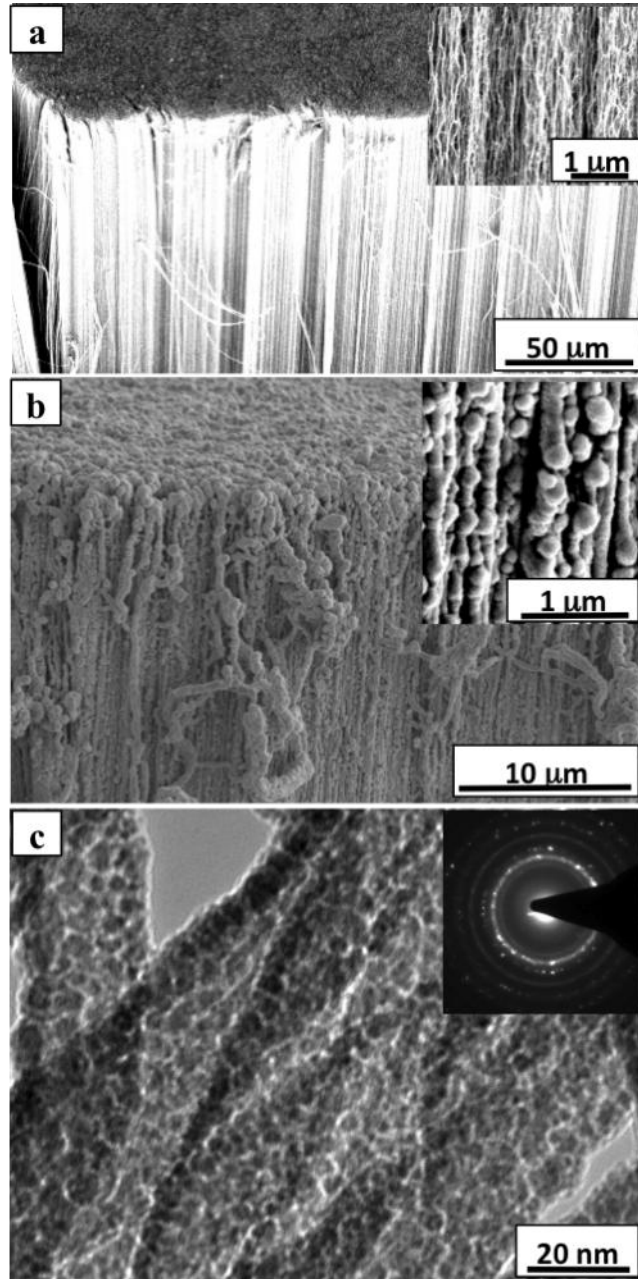


Fig. 1.

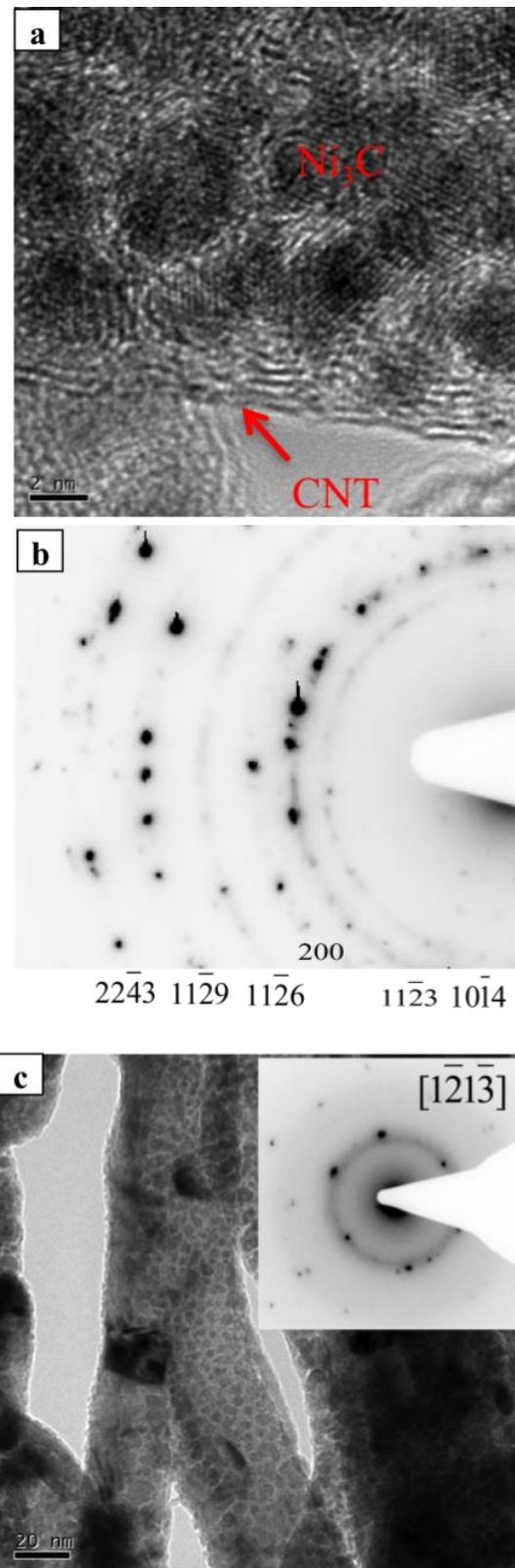


Fig. 2.

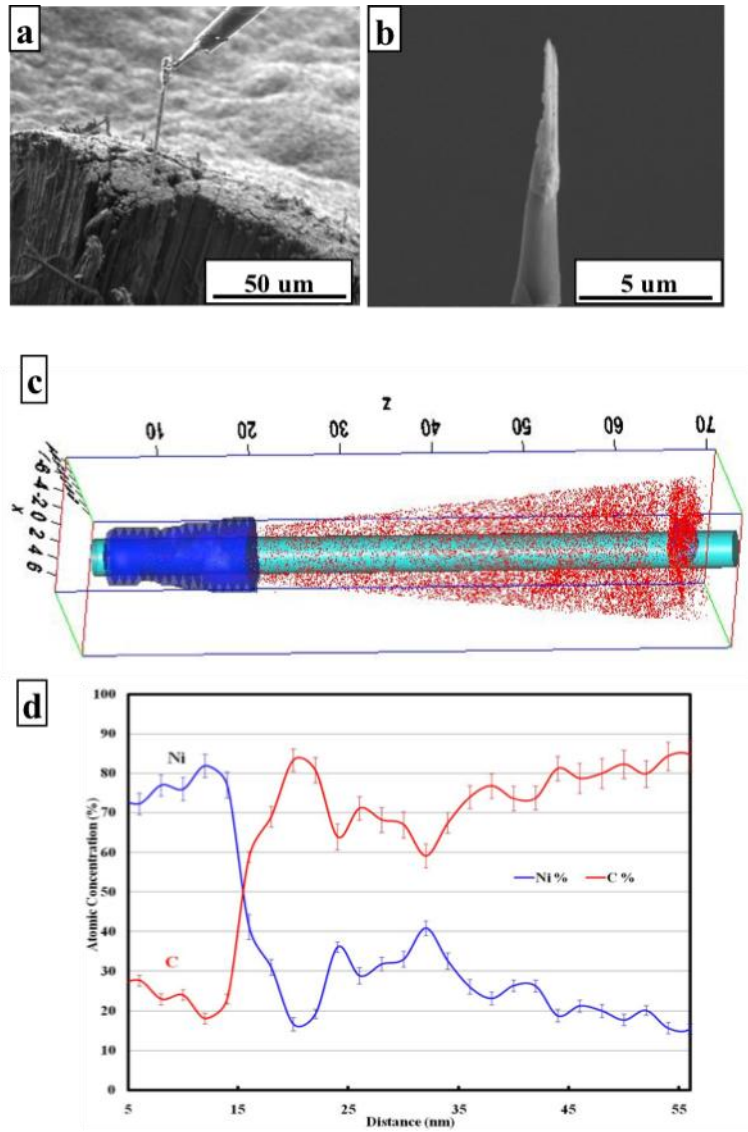


Fig. 3.

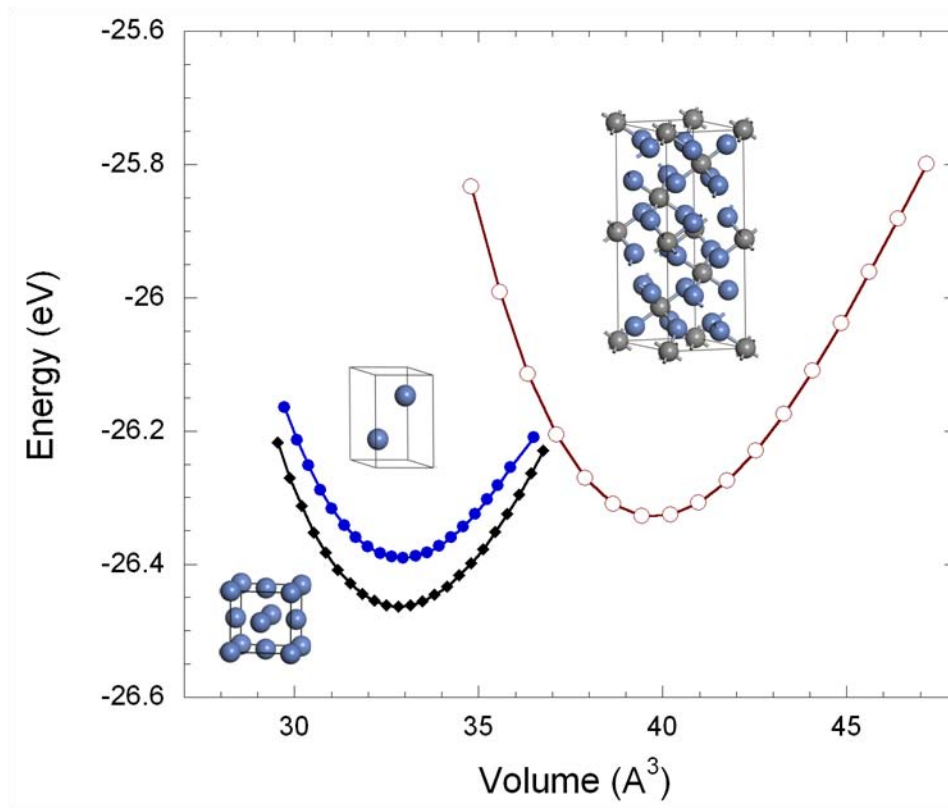


Fig. 4 Energy versus volume curves of HCP Ni, FCC Ni and HCP Ni<sub>3</sub>C calculated using spin polarized periodic planewave DFT with GGA-PBE functional. Open circle: Ni<sub>3</sub>C; filled circle: HCP Ni, filled square FCC Ni. For HCP and FCC Ni, the curves were plotted for 3 Ni atoms and the energy shifted by adding the energy of carbon in the diamond form to be comparable with Ni<sub>3</sub>C. Inset: the unit cell of FCC and HCP Ni, and HCP Ni<sub>3</sub>C. Grey ball: carbon, blue ball: nickel.

Table 1. Comparison of the unit cell parameter of hexagonal Ni<sub>3</sub>C and hexagonal Ni.

	<i>Cell parameter</i>	<i>Angles</i>	<i>Space group</i>	<i>Interlayer distances</i>	<i>TEM measured distance</i>
<i>Ni<sub>3</sub>C (HCP)</i>	4.600/13.016 (4.553/12.920) <sup>a</sup>	90.0/90.0/120.0 (90.0/90.0/120.0) <sup>a</sup>	<i>R-3C</i> (167)	10-14: 2.52 11-23: 2.03 11-26: 1.57	2.5 2.0 1.5
<i>Ni (HCP)</i>	2.488/4.099 (2.48/4.08) <sup>b</sup>	90.0/90.0/120.0 (90.0/90.0/120.0)	<i>P6<sub>3</sub>/MMC</i> (194)		

<sup>a</sup> experimental structure from ref. 16.

<sup>b</sup> equilibrium structure from DFT calculations from ref. 22.